

Investigation of GIC effects on core losses in single phase power transformers*

SEYED ALI MOUSAVI¹, GÖRAN ENGDAHL¹, EDRIS AGHEB²

¹Royal Institute of Technology (KTH), Electromagnetic Engineering Department
Teknikringen 33, SE-100 44, Stockholm, Sweden

e-mail: seyedali.mousavi@ee.kth.se

²Norwegian University of Science and Technology (NTNU)
Trondheim N-7491, Norway

e-mail: edris.agheb@ntnu.no

(Received: 02.07.2010, revised: 29.11.2010)

Abstract: This paper presents a method for estimation of core losses in banks of single phase power transformers that are subjected to an injected DC current such as geomagnetically induced currents (GIC). The main procedure of the core loss calculation is to obtain a magnetic flux density waveform in both time and location by using a novel algorithm based on 3D FEM inside the core and then to calculate the loss distribution based on loss separation theory. Also, a simple and effective method is proposed for estimation of losses of asymmetric minor loops by using combination of symmetric loops. The effect of DC biasing on core losses in single phase power transformers is investigated and the sensitivity of core type and material is evaluated. The results show that DC current biasing could increase core losses up to 40 percent or even more.

Key words: power transformers, geomagnetically induced currents, and hysteresis

1. Introduction

Superimposed DC currents in form of geomagnetically induced currents (GIC) can be injected in three phase transformers or banks of single phase transformers with grounded star-connected windings. The frequencies of these currents are very low and they are quasi-DC. GIC current causes the transformer core to be saturated during one of the half cycles of each supply voltage period. It is noticeable that a small DC current, due to the number of winding turns, can create a huge MMF inside the core. This phenomenon has several adverse effects on performance of power transformers such as increasing noise levels, core losses, winding losses and stray losses in tank and metallic constructions. In [3, 11, 12], increased magnetization cur-

*This is extended version of a paper which was presented at the 21st *Symposium on Electromagnetic Phenomena in Nonlinear Circuits*, Essen-Dortmund, 29.06-02.07, 2010.

rent, reactive power demand and stray losses in tank and other parts in the transformer construction are investigated. In this paper, the effect of GIC on core losses of single phase power transformers is considered by using three dimensional finite element methods (FEM).

The main procedure of the core loss calculation is to obtain a magnetic flux density waveform in both time and location by using FEM inside the core and then calculate the loss distribution based on loss separation theory. The novel proposed algorithm in this paper possesses both accuracy and speed of calculation. In the three dimension finite element modelling of the core, both nonlinearity and anisotropy of the laminated electrical steel core are considered. For purpose of better accuracy, the magnetic vector potential with edge-based formulation is used when solving the Maxwell equations of the transformer model.

The static hysteresis loops in the case of DC biasing are asymmetrical; therefore a suggested method is used to calculate the hysteresis losses under this condition. Also the flux density waveforms inside the core are dramatically distorted. That causes an increased amount of eddy currents and excess losses. All these are calculated in an appropriate manner.

The excellent agreement, between measurement results of no-load tests of real power transformers in normal and over-excitation conditions and calculation results, indicate the accuracy of the model.

2. Finite element transformer model

Analysis of the flux density distribution in the core of power transformers for an arbitrary applied voltage is a very complicated electromagnetic problem, because of 3D geometry, non-linear and oriented core material, electrical and magnetic couplings and time dependencies. In the case of evaluating the flux distribution by solving the Maxwell equations in the entire transformer, 3D FEM method is a powerful tool. The huge computation time is, however, its main drawback.

By using the method presented in this paper, the FEM-analysis is only used once, and for arbitrary applied voltages, the previous saved results are used. The main idea of this method is to perform the static analysis several times for different applied currents up to the amount that completely saturates the core (I_{sat}). In each step, applied current, I , total flux linkage per turn that passes through the winding cross section, Ψ , and flux density of each core element, B_i , all over the core are calculated and saved. Then, the relationship between Ψ and flux density of each core element and also between Ψ and the magnetizing current is obtained. Therefore, for specific amount of Ψ , the flux density distribution inside the core can be obtained by curve fitting of the saved data.

It should be considered that the input source is based on voltage. So in the post-process stage, for an arbitrary applied voltage, the flux linkage per turn for a N -turn winding is equal to:

$$\Psi(t) = \frac{1}{N} \int V(t) dt + \Psi_0. \quad (1)$$

During normal excitation and in the steady-state condition, the flux linkage has no DC offset and Ψ_0 is zero. When the transformer is subjected by GIC, a quasi DC current is injected into the transformer winding resulting in a DC offset into the flux linkage, Ψ_0 . The amount of Ψ_0 is determined by the relationship between Ψ and magnetizing current. Therefore, in each time step, the magnetic flux densities of core elements are evaluated based on the relation between Ψ and B that is obtained by the FEM method. Finally, one will get flux density waveform of all core elements. The main privilege of this method is converting the time-dependent nonlinear problem to a static analyses and use of saved results to calculate the distribution of the magnetic flux density for any arbitrary applied voltage. The proposed method results in high calculation speed.

The Maxwell equation under static condition is:

$$\nabla^2 A = -\mu_r \mu_0 J, \quad (2)$$

where μ_r is a tensor for core material:

$$\mu_r = \begin{bmatrix} \mu_{r,x} & 0 & 0 \\ 0 & \mu_{r,y} & 0 \\ 0 & 0 & \mu_{r,z} \end{bmatrix}. \quad (3)$$

For oil and windings, μ_r is a constant with a value equal to 1. Since the analysis is magnetostatic, it is not necessary to set any conductivity to the materials included in the model.

To decrease the simulation volume and time, only one eighth of whole structure is considered, because of the symmetries. Figure 1 illustrates the structure of a 4-limb single phase transformer and the 1/8 applied symmetry. In nodal formulation, the discontinuity of tangential component in heterogeneous medium leads to incorrect results, thus, the edge-element formulation is used in this paper to avoid erroneous results.

Meshing of the core and also the inner volume of the transformer are performed by pyramid elements and the winding by brick elements.

The iron tank of the transformer is modeled as boundary with perpendicular flux boundary conditions. Appropriate boundary conditions, flux normal and flux parallel, are assigned on cutting faces of 1/8 symmetry model.

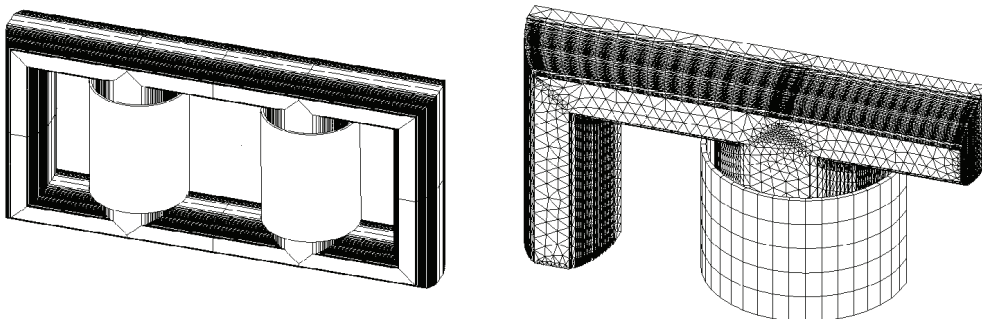


Fig. 1. The single phase 4-limb power transformer and its FEM model with one-eighth symmetry, the mesh of oil region is not shown in this figure

In each step of the finite element analysis, a current density with uniform distribution is applied to the winding. Since, in single phase transformers, inverting the direction of the applied current brings about the reverse direction of the magnetic flux, it is necessary to only do the analyses for positive currents, and it causes the deduction of the simulation time. Thus, different current magnitudes between zero and I_{sat} are applied as the inputs. According to these inductions, the spatial distribution of the magnetic flux density in the core is calculated. The FEM procedure is depicted in Figure 2.

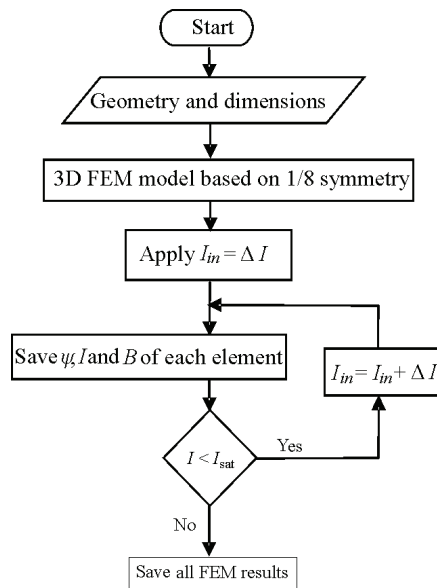


Fig. 2. The procedure of FEM modeling

In this stage, the hysteresis effect is neglected, but in the loss calculation stage, it is completely considered even for minor loops. Then by using the stored values of B and their relationship with injected currents, the waveform of spatial distribution of magnetic flux density is obtained. In each step, to solve the nonlinear equations, the repetitive Newton-Raphson method is used.

In Figure 3, a brief summary of the proposed method is illustrated.

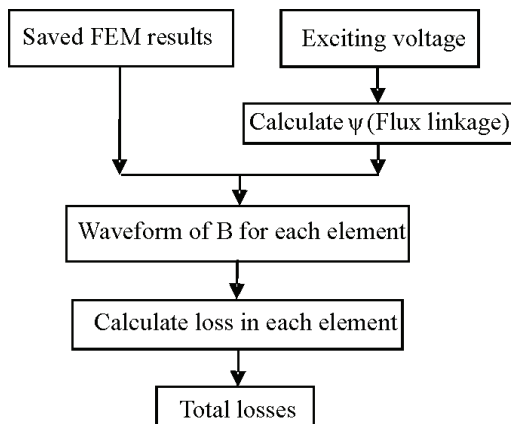


Fig. 3. The procedure of post-processing core loss calculation

3. Core loss calculation

According to a suggested hypothesis regarding loss separation theory, core losses in laminated steels consist of three components [5]:

$$P_t = P_h + P_e + P_{exc}, \quad (4)$$

where P_t is total losses, P_h is static hysteresis losses, P_e is classic eddy current loss and P_{exc} is excess eddy current losses.

Static hysteresis losses represent the area of the hysteresis cycle obtained at very low frequencies. They result from the behaviour at a microscopic scale of the magnetic structure of the material. The hysteresis energy loss, P_h , is independent of the magnetization rate [1]. But, it depends on magnetic flux density waveform. There are several models and algorithms for predicting hysteresis trajectory and calculating static hysteresis losses [4, 6, 8, 9], and the most well known of them are Preisach [9] and Jiles-Atherton [7, 8]. However, in addition to the fact that these models have some intrinsic restrictions, they need a relatively heavy computational process [2, 10]. Therefore, using such methods with three dimensional FEM in this work that deals with tens of thousands of core elements, will require too much computational time and memory.

Since the aim of this paper is to estimate average power losses, faster and simpler ways with enough accuracy are applicable. For symmetric static hysteresis loops, the relation between maximum flux density and hysteresis loss per unit mass, P_h , can be described by:

$$\begin{aligned} P_h &= K_h B_{\max}^{a \cdot B_{\max}^2 + b \cdot B_{\max} + c} f & B_{\max} < B_{\max, major} \\ P_h &= P_{h, major} & B_{\max} \geq B_{\max, major}, \end{aligned} \quad (5)$$

where B_{\max} is the maximum flux density for symmetric hysteresis loops, K_h , a , b and c are constant coefficients and f is the main frequency. In regions with flux densities higher than the maximum flux density of the major loop, $B_{\max} \geq B_{\max, major}$, the hysteresis loop trajectory is reversible [7]. Therefore, the loop area of that region is considered zero. However, in the case of DC magnetization, one faces unsymmetrical flux density waveforms that cause unsymmetrical minor loops like that shown in Fig. 4.

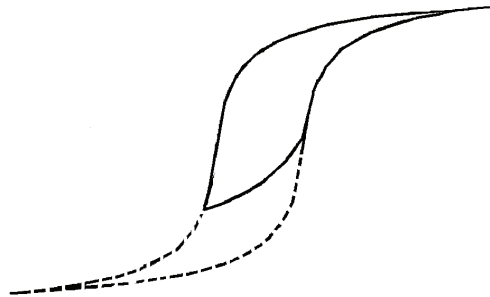


Fig. 4. The sample of asymmetric hysteresis loop that is caused by GIC

The idea of the proposed method is to estimate the area of those unsymmetrical loops by a combination of symmetrical ones. For instance, according to Figure 5, one can assume that:

$$P_h = (S_1 + S_2) f = \left(\frac{(2S_1 + S_2) - S_2}{2} + S_2 \right) f = 0.5((2S_1 + S_2) + S_2). \quad (6)$$

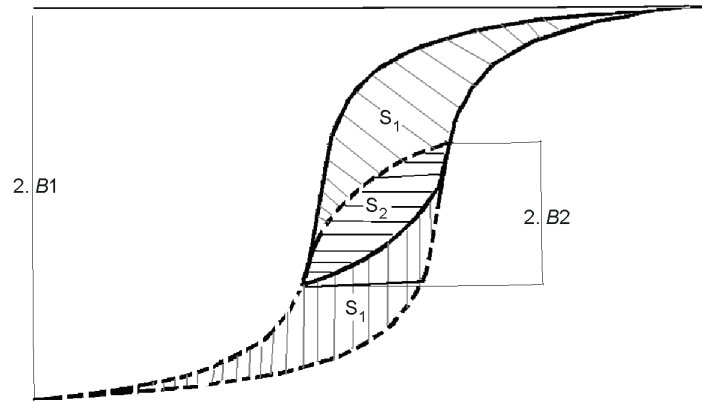


Fig. 5. The idea for estimation of area of asymmetric loop with combination of symmetric ones

Then

$$P_h = 0.5 P_{h, B_1} + 0.5 P_{h, B_2}. \quad (7)$$

For loops with a turning point above zero, a similar method can be applied. Also for symmetrical minor loops with their centers are not in the origin, we assume that the loss is equal to the loss of the symmetrical minor loops with its center placed in the origin with the same flux density variation. This method may be not very exact, but it seems reasonable for estimation of core losses in the case of GIC. The authors of this paper will improve and verify it by measurements on different classes of materials at future papers.

The variation of magnetic flux in conductive media causes induction of eddy currents perpendicular to the flux direction. These currents create ohmic losses.

The instantaneous classical power loss per unit mass, due to eddy currents $P_e(t)$, can be defined as [1]:

$$P_e(t) = \frac{1}{\rho} \frac{1}{12} \sigma d^2 \left(\frac{dB}{dt} \right)^2, \quad (8)$$

where σ is the conductivity of the magnetic material and d and ρ are the thickness and density of lamination steel, respectively.

The total core losses are greater than the summation of hysteresis and classic eddy current losses. This gap is called excess losses that result from local eddy currents created by domain wall motion in alternating magnetic flux. The expression is derived from Bertotti's statistical theory of losses, which provides, for a wide class of materials [1], the equation:

$$P_{exc}(t) = K_{exc} \left| \frac{dB}{dt} \right|^{3/2}. \quad (9)$$

Where $P_{exc}(t)$ is the instantaneous excess power loss per unit mass and K_{exc} is the constant excess loss coefficient.

Then, the total power loss for an arbitrary flux density waveform can be obtained by:

$$P = P_h + \frac{1}{T} \int \frac{1}{\rho} \frac{\sigma d^2}{12} \left(\frac{dB(t)}{dt} \right)^2 dt + \frac{1}{T} \int K_{exc} \left(\left| \frac{dB}{dt} \right| \right)^{1.5} dt. \quad (10)$$

The classical eddy current losses are calculated by using the material characteristics of electrical steel. The coefficients of hysteresis and excess losses can be extracted from data of core losses with sinusoidal excitation for at least two different frequencies and four different magnetic flux densities less than the maximum flux density of the major magnetization loop. Such data usually exists in datasheets from steel manufacturers or can easily be measured.

For sinusoidal flux density waveform, expression (10) becomes [1]:

$$P_{sin} = K_h B_{max}^{a \cdot B_{max}^2 + b \cdot B_{max} + c} f + K_e B_{max}^2 f^2 + 8.76 \times K_{exc} B_{max}^{1.5} f^{1.5}, \quad (11)$$

where

$$K_e = \frac{\sigma \pi^2 d^2}{6\rho}, \quad (12)$$

K_{exc} can be obtained from each pair of core losses with the same flux density at different frequencies. When having K_e and K_{exc} , the hysteresis losses can be estimated based on core loss data. The coefficients of hysteresis losses are then obtained from the hysteresis losses in four different flux densities, by solving the linear equation system, below:

$$\log\left(\frac{P_{h,i}}{f}\right) = \log(K_h) + a \cdot B_{max,i}^2 \cdot \log(B_{max,i}) + b \cdot B_{max,i} \cdot \log(B_{max,i}) + c \cdot \log(B_{max,i}) \quad i=1, 2, 3, 4. \quad (13)$$

4. Validation

The proposed core loss calculation method has been applied on several power transformers including 2-limb, 3-limb and 4-limb types. The rated power and voltage of tested transformers are given in Table 1. In Tables 2 to 5, comparisons between measurements and calculations are shown. The excellent agreement between measurements and calculation for both normal and over-excitation operation conditions demonstrates the accuracy of the FEM model and the loss calculation method. Consequently, it is feasible at estimation of losses in the case of DC magnetization.

Table 1. Rated power and voltage of single phase transformers under test

	2-limb	3-limb	4-limb
Rated voltage (kV)	235.3/15.75	235.3/135.3	235.3/135.3
Power (MVA)	100	166.7	200

Table 2. 2-limb single phase transformer material M5;
average flux density in 100% voltage = 1.703, 50 Hz

U/U_n %	B_{\max} (T)	Test (kW)	Proposed method (kW)	Error (%)
110	1.87	78.73	79.08	0.4
100	1.70	55.99	55.99	0.4
90	1.53	40.25	40.25	0.49

Table 3. 3-limb single phase transformer material M5;
average flux density in 100% voltage = 1.704, 50 Hz

U/U_n %	B_{\max} (T)	Test (kW)	Proposed method (kW)	Error (%)
110	1.87	62.04	63.18	1.80
100	1.70	45.96	45.97	0.02
90	1.53	35.12	34.44	1.90

Table 4. 4-limb single phase transformer material M5;
average flux density in 100% voltage = 1.661, 50 Hz

U/U_n %	B_{\max} (T)	Test (kW)	Proposed method (kW)	Error (%)
110	1.83	156.09	155.4	0.44
100	1.66	113.7	112.68	0.89
90	1.50	82.56	83.47	1.10

Table 5. 4-limb single phase transformer material M5;
average flux density in 100% voltage = 1.661, 60 Hz

U/U_n %	B_{\max} (T)	Test (kW)	Proposed method (kW)	Error (%)
110	1.83	198.7	199.12	0.21
100	1.66	150.66	148.44	1.40
90	1.50	109.06	110.35	1.10

5. Analysis of results

In order to analyze the effects of GIC on core losses, three real power transformers, a 2 limb, 3 limb and a 4 limb transformer with both M5 and HIB core steel have been modeled. In the model, the supply voltage across the transformer winding is assumed constant, but in practice, it will be declined due to the voltage drop created by the dramatically increase of the magnetization current and the other losses in the transformer. Thus, the results of losses for higher DC offsets may be a little bit over-estimated.

For maximum efficiency, power transformers are designed to work near the knee point of the saturation curve. This leads to a high sensitivity to DC magnetization. Figure 6 shows how a DC offset of the average flux densities would change according to an injected DC current. It can be concluded that single phase power transformers are very vulnerable to small amounts of DC current. On the other hand, by increasing the number of the limbs, their sensitivity of the DC component of the average flux density will increase.

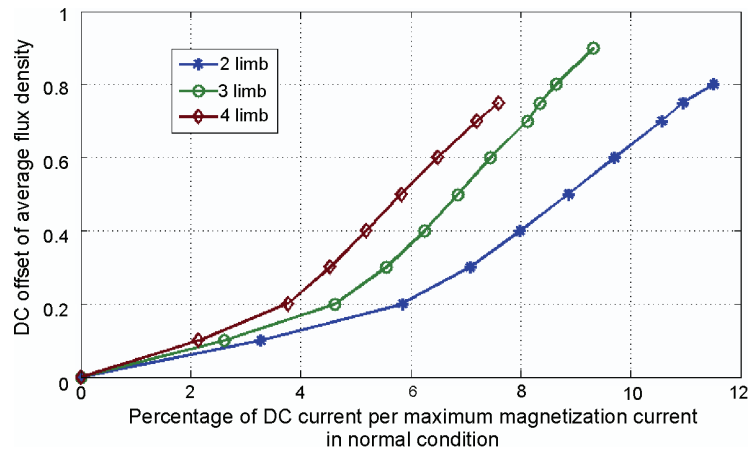


Fig. 6. Relationship between DC current and DC offset of average flux density for various core types, with material M5

The results of the modeling reveal that an increase in the DC offset to around 0.6 T can increase the core losses with up to nearly 50%. This amount of DC offset can appear by small values of GIC. The increase of core losses corresponding to the DC offsets for all core types is shown in Figure 7. The various core types show no noticeable difference in increased core losses for the same DC offset of the average flux density.

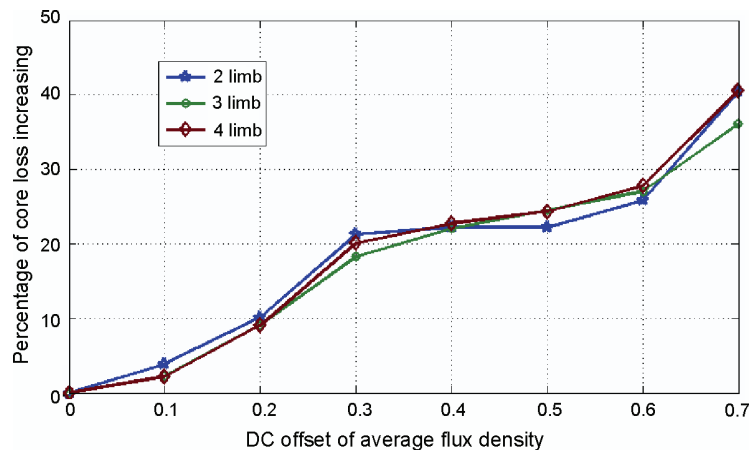


Fig. 7. Relationship between DC offset and core loss increasing for various core types, with material M5

Under normal condition, a core made of HIB electrical steel has lower losses and higher permeability than one made of M5 with the same design. As it is depicted in Figures 8 and 9, HIB type is more sensitive to the magnitude of a DC current such that M5 type can manage a higher DC current with the same losses.

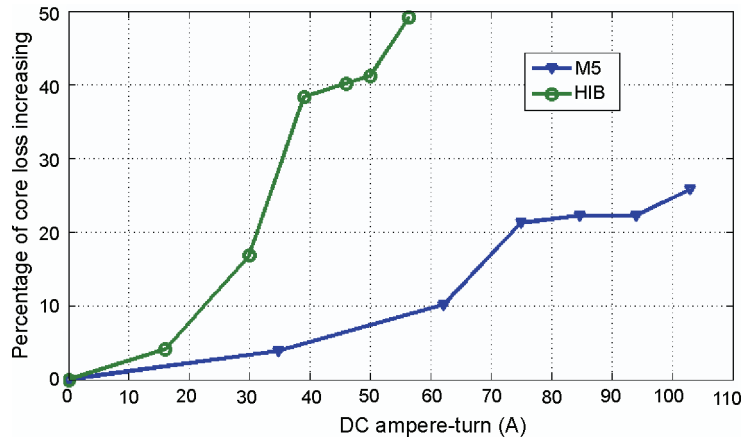


Fig. 8. Comparison between HIB and M5 in percentage of core loss increasing for 2 limb transformer

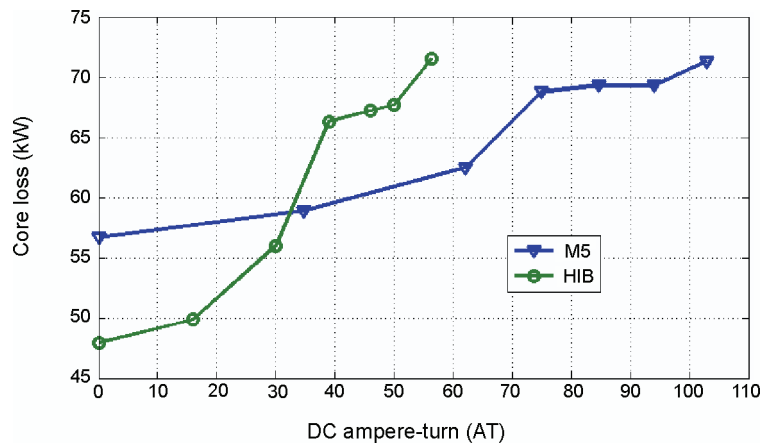


Fig. 9. Comparison between HIB and M5 in core loss increasing for 2 limb transformer

The investigation of the contribution of the losses discloses that static hysteresis losses play main role regarding the increase of losses for low DC offsets, but when raising the DC offset, the rate of hysteresis losses increment becomes low and the rate dependent losses (classical and excess eddy current losses) increase due to growth of higher harmonics in the flux density waveforms inside the core. The contributions to the losses are shown in Figure 10.

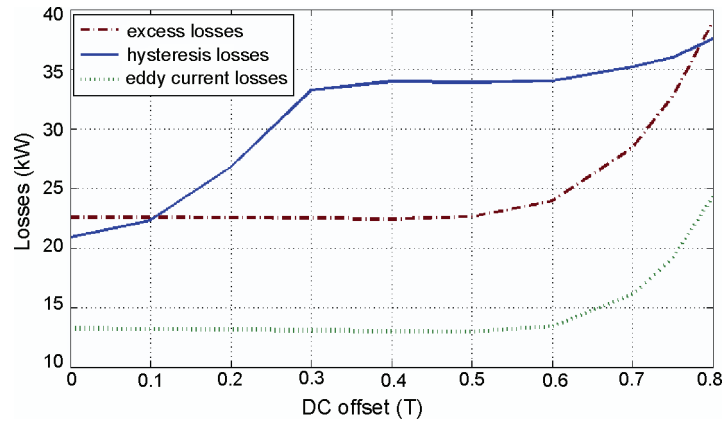


Fig. 10. Contribution of losses respect to DC offset for 2 limb transformer with M5 material

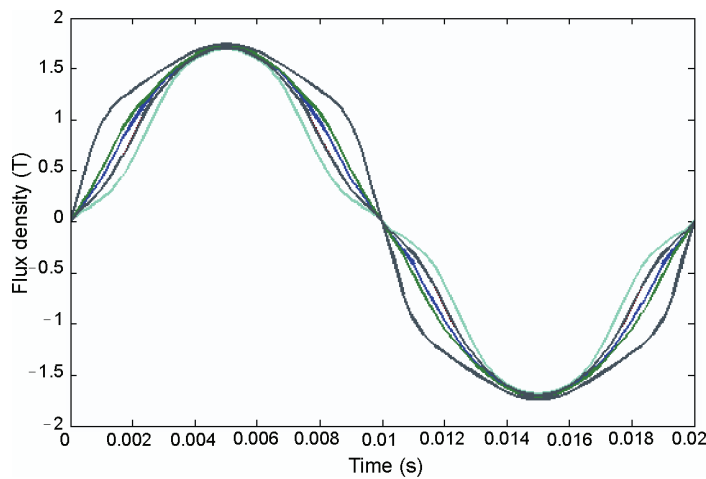


Fig. 11a. Flux density waveforms for some points of 2 limb core with M5 material without DC offset

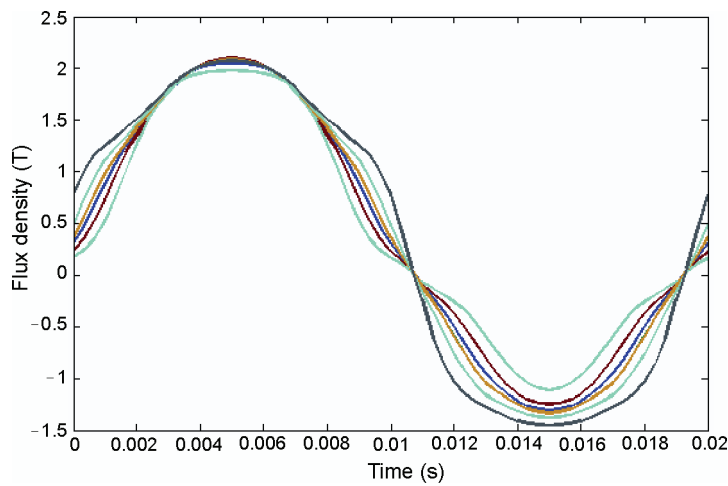


Fig. 11b. Flux density waveforms for some points of 2 limb core with M5 material with 0.4 T average DC offset

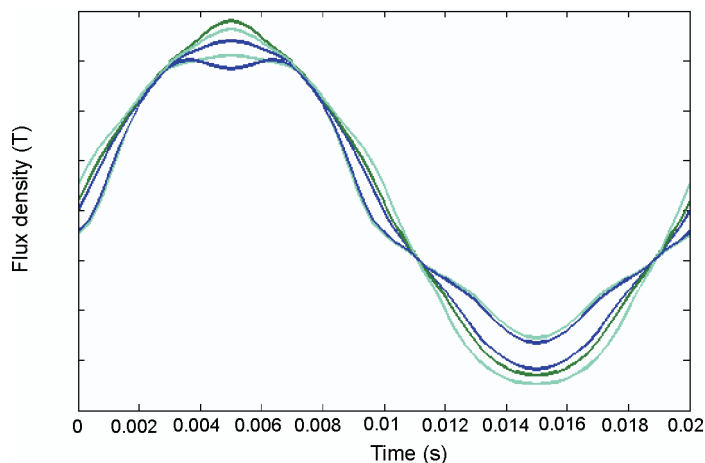


Fig. 11c. Flux density waveforms for some points of 2 limb core with M5 material with 0.6 T average DC offset

As was explained and is shown in this figure, for low DC offsets, excess losses are higher than the other ones, but increasing this component, the static hysteresis losses will be the dominant mechanism in the core. On the other hand, up to a DC offset of 0.6 T, the excess and eddy current losses are almost constant, but for a DC magnitude higher than 0.6 T, the start increase sharply. To get a better concept of the flux density behavior, the waveform of B at several points of the core of the 2 limb transformer with 0 T, 0.4 T and 0.6 T DC offset is shown in Fig. 11.

6. Conclusion

In this paper, based on 3D FEM, a novel method is presented to calculate the core losses for banks of single phase power transformers when subjected DC currents, such as GIC. Also, a simple and effective method is proposed for the calculation of hysteresis losses in the case of asymmetric minor loops. In order to verify the accuracy of the presented approach, the simulation results are compared with no-load tests of real power transformers in normal and over-excitation conditions. The excellent agreement between the results demonstrates the accuracy of the FEM model and the losses calculation method. Consequently, it is feasible at estimation of losses in the case of DC magnetization.

The results of modeling of real power transformers prove that the small amounts of the DC currents will increase the core losses considerably. The effects of core type and material on increasing of losses are investigated in this paper. Also to have a better understanding of the mechanism of losses increasing, the contributions of static hysteresis, eddy current and excess losses, are evaluated.

References

- [1] Barbisio E., Fiorillo F., Ragusa C., *Predicting loss in magnetic steels under arbitrary induction waveform and with minor hysteresis loops*. IEEE Transaction on Magnetics 40(4): 1810-1819 (2004).

-
- [2] Benabou A., *Comparison of the Preisach and Jiles-Atherton models to take hysteresis phenomenon into account in finite element analysis*. COMPEL: The International Journal for Computation and Mathematics in Electrical and Electronic Engineering 3: 825-834 (2004).
 - [3] Biro O., Buchgraber G., Leber G., Preis K., *Prediction of Magnetizing Current Wave-Forms in a Three-Phase Power Transformer Under DC Bias*. IEEE Transaction on Magnetics 44(6): 1554-1557 (2008).
 - [4] Guerra F.C.F., Mota W.S., *Magnetic core model*. IET Sci. Meas. Technology 1(3): 145-151 (2007).
 - [5] Bertotti G., *Hysteresis in magnetism*. Academic Press (1998).
 - [6] Hodgdon M.L., *Applications of a theory of ferromagnetic hysteresis*. IEEE Transaction on Magnetics 24(1): 218-221 (1988).
 - [7] Jiles D.C., *Introduction to magnetism and magnetic materials*. Chapman and Hall, London (1991).
 - [8] Jiles D.C., Atherton, D.L., *Theory of ferromagnetic hysteresis*. Journal of Magnetic Materials 61: 48-60 (1986).
 - [9] Naidu S.R., *Simulation of the hysteresis phenomenon using Preisach's theory*. IEE Proc. A, Phys. Sci. Meas. Instrum. Manag. Edu. 137(2): 73-79 (1990).
 - [10] Philips D.A., Duprc L.R., Melkebeek J.A., *Comparison of Jiles and Preisach hysteresis models in magnetodynamics*. IEEE Transactions on magnetics: 3551-3553 (1995).
 - [11] Price P.R., *Geomagnetically induced current effects on transformers*. IEEE Transaction on Power Delivery. 17(4): 1002-1008 (2002).
 - [12] Yao Y., Koh C.S., Ni G., Xie D., *3-D nonlinear transient eddy current calculation of online power transformer under DC bias*. IEEE Transaction on Magnetics 41(5): 1840-1843 (2005).